Molecular Cancer Therapeutics

Direct Binding of Arsenic Trioxide to AMPK and Generation of Inhibitory Effects on Acute Myeloid Leukemia Precursors

Elspeth M. Beauchamp[1,2,3], Ewa M. Kosciuczuk[1,2], Ruth Serrano[1,2], Dhaval Nanavati[1], Elden P. Swindell[1,4,5], Benoit Viollet[6], Thomas V. O'Halloran[1,4,7], Jessica K. Altman[1,2,3], and Leonidas C. Platanias[1,2,3]

Abstract

Arsenic trioxide (As_2O_3) exhibits potent antineoplastic effects and is used extensively in clinical oncology for the treatment of a subset of patients with acute myeloid leukemia (AML). Although As_2O_3 is known to regulate activation of several signaling cascades, the key events, accounting for its antileukemic properties, remain to be defined. We provide evidence that arsenic can directly bind to cysteine 299 in AMPKα and inhibit its activity. This inhibition of AMPK by arsenic is required in part for its cytotoxic effects on primitive leukemic progenitors from patients with AML, while concomitant treatment with an AMPK activator antagonizes *in vivo* the arsenic-induced antileukemic effects in a xenograft AML mouse model. A consequence of AMPK inhibition is activation of the mTOR pathway as a negative regulatory feedback loop. However, when AMPK expression is lost, arsenic-dependent activation of the kinase RSK downstream of MAPK activity compensates the generation of regulatory feedback signals through phosphorylation of downstream mTOR targets. Thus, therapeutic regimens with As_2O_3 will need to include inhibitors of both the mTOR and RSK pathways in combination to prevent engagement of negative feedback loops and maximize antineoplastic responses. *Mol Cancer Ther; 14(1); 202–12. ©2014 AACR.*

Introduction

Arsenic trioxide (As_2O_3) has been used for centuries as a medicinal compound for the treatment of a variety of medical conditions (1). Currently, arsenic trioxide is approved by the FDA for the treatment of relapsed acute promyelocytic leukemia (APL), a subtype of AML (2, 3). Trivalent arsenic is the species found in medicinal arsenic compounds, including As_2O_3. Its major mechanism of action in cells is to bind to thiol groups in the cysteines of proteins, resulting in modulation of their function and thus affecting cellular signaling pathways (4–6). There is also evidence for disease-specific mechanisms of action of As_2O_3 in APL through binding to and degradation of the PML–RAR fusion protein (7). In fact, previous studies have established that As_2O_3 specifically binds to the PML zinc finger domain at cysteine residues leading to a shift in secondary structure, which leads to increased sumolyation and degradation (8).

Treatment of malignant cells with As_2O_3 has been shown to result in modulation of many other signaling pathways. Besides PML–RAR, arsenic has been also shown to cause degradation of fusion proteins that regulate downstream signals in different leukemias (9, 10). As_2O_3 has been also shown to bind directly to IKK-β and inhibit NF-κβ signaling (11). Multiple studies have established potent effects of arsenic on MAPK pathways. The treatment of different leukemia cell types with As_2O_3 results in activation of p38 MAPK (12). In addition, inhibition of p38 MAPK or its downstream effectors enhances the cytotoxic effects of As_2O_3 (13–15), suggesting that this cascade is engaged and acts as negative feedback regulatory pathway. ERK has also been shown to be activated by As_2O_3 and may be important for the induction of autophagy, as well as lead to the degradation of the PML protein (16, 17). More recently, As_2O_3 was shown to activate RSK1 in a negative feedback manner in leukemia cells (18). Others studies have shown that the JNK kinase pathway is engaged by As_2O_3 and such activation promotes apoptosis of leukemia cells (19–21). There is also evidence that arsenic affects the Hedgehog pathway, which can lead to either cell death or cell proliferation, depending on the GLI isoform inhibited (22–24). Thus, engagement of various signaling cascades by As_2O_3 results in opposing responses, depending on the context and cellular subtype.

The major cellular function of AMPK is to regulate energy homeostasis (25). When cellular ATP levels drop, AMPK is phosphorylated by the upstream kinases LKB1 and CAMKK at residue Thr172, resulting in its activation (26–29). Downstream targets of AMPK include ACC, ULK, and mTORC1, which act as mediator/

[1]Robert H. Lurie Comprehensive Cancer Center of Northwestern University, Chicago, Illinois. [2]Division of Hematology/Oncology, Department of Medicine, Feinberg School of Medicine, Northwestern University, Chicago, Illinois. [3]Division of Hematology-Oncology, Department of Medicine, Jesse Brown VA Medical Center, Chicago, Illinois. [4]Chemistry of Life Processes Institute, Northwestern University, Evanston, Illinois. [5]Department of Chemical and Biological Engineering, Northwestern University, Evanston, Illinois. [6]Institut Cochin, Université Paris Descartes, CNRs (UMR8104) and INSERM U1016, Paris, France. [7]Department of Chemistry, Northwestern University, Evanston, Illinois.

Note: Supplementary data for this article are available at Molecular Cancer Therapeutics Online (http://mct.aacrjournals.org/).

Corresponding Author: Leonidas C. Platanias, Robert H. Lurie Comprehensive Cancer Center and Jesse Brown VA Medical Center, 303 East Superior Street, Lurie 3-125, Chicago, IL 60611. Phone: 312-503-4755; Fax: 312-908-1372; E-mail: l-platanias@northwestern.edu

doi: 10.1158/1535-7163.MCT-14-0665-T

effectors to metabolism and autophagy (30–32). AMPK can inhibit mTORC1 by directly phosphorylating TSC2 and Raptor, which affects mTORC1 complex formation and activation (33).

There has been a major interest for the use of As_2O_3 and other medicinal arsenic compounds in the treatment of multiple cancer types, including myeloid leukemias (3, 6). However, to date, arsenic has not shown significant clinical activity as a single agent outside of APL (3). A major reason for this may be the activation of negative feedback pathways during treatment of cells with As_2O_3. Previous work from our group has established that the mTOR pathway is activated by As_2O_3 in myeloid leukemia cells and acts as a negative feedback regulatory loop; however, the mechanism is unknown (34). In the current study, we sought to examine the effects of As_2O_3 on AMPK. It has been previously shown that oxidation of specific cysteine residues in AMPK is important for its activation (35), and therefore we hypothesized that arsenic can bind to those cysteine residues and prevent activation of AMPK, leading to the activation of mTOR.

Materials and Methods

Cells and reagents

The U937 cell line was obtained from ATCC in September of 2013. The Kasumi-1 cell line was obtained from ATCC in September 2011. Both cell lines were frozen at low passage (2–3 passages after receipt) in liquid nitrogen and experiments were conducted on cells passaged for a total of no more than 1 month after resuscitation and therefore cells did not need to reauthenticated. AMPKα1/2 WT and AMPKα1/2$^{-/-}$ immortalized mouse embryonic fibroblasts (MEF) were as previously described (36) and were grown in DMEM supplemented with 10% FBS. Cells were verified for AMPKα knockout by Western blot analysis (see Supplementary Fig. S1A). Kasumi-1 cells were cultured in ATCC-modified RPMI1640 supplemented with 20% FBS. U937 cells were cultured in RPMI1640 supplemented with 10% FBS. As_2O_3 was purchased from Sigma. PP242 was purchased from Chemdea. A769662 was purchased from Santa Cruz Biotechnology and Chemietek. BI-D1870 was purchased from Symansis.

Cell lysis and immunoblotting

Cells were lysed in phospho-lysis buffer (50 mmol/L HEPES, pH 7.9; 150 mmol/L NaCl; 4 mmol/L sodium pyrophosphate; 1 mmol/L EDTA, pH 8.0; 10 mmol/L NaF; 0.5% Triton-X 100; 10% glycerol) with 1 mmol/L phenylmethylsulfonylfluoride, protease inhibitor cocktail set V (EMD Millipore), and phosphatase inhibitor cocktail set I (EMD Millipore) added freshly. Cells were briefly sonicated, centrifuged, and then snap frozen in liquid nitrogen. Upon thawing, cell lysates were subjected to SDS-PAGE and then transferred to an Immobilon-P membrane (Millipore). Membranes were then subjected to blocking in 5% nonfat dry milk in 1× TTBS (20 mmol/L Tris-HCL, pH 7.5; 150 mmol/L NaCl; and 0.5% Tween 20) for 1 hour. All antibodies were purchased from Cell Signaling Technology except the antibodies against GAPDH (Millipore), and HSP 90α/β (Santa Cruz Biotechnology). Primary antibodies were added to the membrane in 1× TTBS for 2 hours or overnight. The membrane was then washed 3 times in 1× TTBS and horseradish peroxidase (HRP)-linked anti-rabbit (GE Healthcare) or anti-mouse secondary antibody (Bio-Rad) was added for 1 hour. Blots were washed 3 times in 1× TTBS and then developed using Amersham ECL Western Blotting Detection Reagent (GE Healthcare Life Sciences) or Immobilon Western Chemiluminescent HRP Substrate (Millipore), as per the manufacturer's instructions. Chemiluminescence was detected using autoradiography film. Films were digitally scanned with Adobe Photoshop CS5 using a Canon CanoScan 8800F scanner.

Streptavidin pulldowns

Cells were treated with an arsenic–biotin conjugate (As-Biotin; CAS Number: 212391-23-6, Toronto Research Chemicals, Inc) at a final concentration of 20 μmol/L for 2 hours. This compound has been previous used to isolated arsenic binding proteins as it will bind to thiol groups (6, 8, 37, 38). After lysis in phospho-lysis buffer, 500 μg of protein was diluted in buffer and the arsenic–protein complexes were then isolated with streptavidin agarose beads by tumbling at 4°C overnight (Invitrogen Life Technologies). For recombinant protein, purified AMPKα1 subunit (Novus Biologicals) or the active holoenzyme containing AMPKα1/β1/γ1 (SignalChem) protein was incubated for 30 minutes with As-Biotin at 30°C. The arsenic–protein complex was then isolated with streptavidin agarose beads at 4°C for 1 hour (Invitrogen Life Technologies). The beads were washed 3 times with phospho-lysis buffer not containing Triton-X 100. The samples were then boiled for 5 minutes at 95°C in 2× Laemmli sample buffer and subject to SDS-PAGE. Immunoblotting was performed as described above.

Construction of AMPKα1-mutant construct

The pECE-AMPKα1 WT construct was kindly provided by Dr. Anne Brunet and Bethany E Schaffer (Stanford University, Stanford, CA). The cysteine residues at 299 and 304 were both mutated to alanine using the following mutagenesis primers: forward, CTATTCCAGAAGTAGTCAGGAGGCTTTTTTGGAGGAG; reverse, CTCCTCCAAAAAA GCCTCCTCACTACTTCTGGAATAG. Mutations using QuickChange Lightning Site-Directed Mutagenesis Kit (Agilent Technologies) were performed as per the manufacturer's protocol. All cloning products were sequenced for verification. For streptavidin pull-down experiments, HEK293 cells were transfected with AMPKα1 using Fugene HD Reagent (Promega) according to the manufacturer's instructions. Streptavidin pulldowns were performed as described above. HA-expressed proteins were detected by Western blot analysis using an HA antibody (Covance).

Kinase assays

Ten nanograms of the fully active holoenzyme AMPKα1/β1/γ1 (SignalChem) protein was incubated for 30 minutes with As_2O_3, compound C, or As-Biotin at 30°C with the doses indicated. A total of 150 mmol/L of ATP, 50 mmol/L DTT, kinase reaction buffer, and 2 μg/mL of SAMStide substrate were added to the drug/enzyme mixture and incubated for 1 hour at 30°C. A no enzyme control was used for a background measurement. Activity of AMPK was measured as the amount of ADP consumed during the reaction using the ADP-Glo Kinase Assay from Promega according to the manufacturer's instructions.

Mass spectroscopy

The arsenic–protein complex was isolated as described above. The beads were washed three times with 100 mmol/L ammonium bicarbonate and then digested with sequencing grade trypsin (Promega). After digestion beads were washed three times with 100 μL of 0.1% formic acid. All the washes were pooled and dried *in vaccuo*. After drying, the peptides were suspended in 5%

acetonitrile and 0.1% formic acid. The samples were loaded directly onto a 10 cm long, 75-μm reversed-phase capillary column (ProteoPep II C18, 300 Å, 5 μm size, New Objective) and separated with a 100-minute gradient from 5% acetonitrile to 100% acetonitrile on a Proxeon Easy n-LC II (Thermo Scientific). The peptides were directly eluted into an LTQ Orbitrap Velos mass spectrometer (Thermo Scientific) with electrospray ionization at 350 nL/minute flow rate. The mass spectrometer was operated in data-dependent mode, and for each MS1 precursor ion scan the ten most intense ions were selected from fragmentation by collision-induced dissociation. The other parameters for mass spectrometry analysis were: resolution of MS1 was set at 60,000, normalized collision energy 35%, activation time 10 ms, isolation width 1.5, and the +1 and +4 and higher charge states were rejected.

The data were processed using PD 1.4 (Proteome Discoverer, version 1.4, Thermo Scientific) and searched using SEQUEST HT search algorithm as in PD 1.4. The data were searched against *Homo sapiens* reference proteome downloaded from uniprot.org (version 2013_7). The other parameters were as follows: (i) enzyme specificity: trypsin; (ii) fixed modification: cysteine carbamidomethylation; (iii) variable modification: methionine oxidation and As-Biotin modification at cysteine; (iv) precursor mass tolerance was ±10 ppm; and (v) fragment ion mass tolerance was ±0.8 Da. The spectrum of As-biotin–modified peptide was manually validated. A corresponding spectrum and table of matching ions are shown in Supplementary Fig. S2.

Cell viability assays

Cellular viability was assessed by triplicate plating at a density of 500 to 2,000 cells/well, depending on the cell line, in a 96-well plate. As_2O_3, PP242, BI-D1870, or A769662 alone or in combination at varying concentrations or vehicle alone (PBS or DMSO) were added to cells in standard growth media for that cell line once the cells had attached for adherent cells or 2 hours after plating for suspension cells. Viable cells were quantified using 20 μL WST-1 Reagent (Roche) according to the manufacturer's protocol after 4 days. IC_{50} and confidence interval (CI) values were calculated using Compusyn to determine whether drug interactions were additive, synergistic, or antagonistic (39).

Clonogenic leukemic progenitor assays in methylcellulose

These assays were performed essentially as in our previous studies (15, 33). Peripheral blood or bone marrow samples were obtained from patients with AML after obtaining informed consent approved by the Institutional Review Board of Northwestern University (Chicago, IL). Mononuclear cells were isolated by Ficoll–Hypaque (Sigma Aldrich) sedimentation. To assess the effects of drugs on leukemic progenitor (CFU-L) colony formation, cells were plated in methylcellulose (MethoCult H4534 Classic without EPO, Stem Cell Technologies).

RNAi targeting

Nontargeting control and AMPKα1 siRNA were purchased from Dharmacon RNAi Technologies. Amaxa Nucleofector Kits (Lonza) were used for the transfection of cell lines. For U937 cells, Kit C was used with program W-001 and for Kasumi-1, Kit V was used with program P-019 on the Nucleofector 2b Device. For patient samples, siRNA knockdowns were performed using TransIT-TKO as recommended by Mirus Bio LLC. Cells were then plated in methylcellulose and assessed for their ability to form CFU-L as described above.

Immunohistochemistry

Tumor samples from mice were formalin-fixed and embedded in paraffin. The Robert H Lurie Comprehensive Cancer Center Pathology Core Facility performed the slide preparation and staining. Slides were stained with hematoxylin and blued in 1% ammonium hydroxide, dehydrated, and mounted for histologic analysis. TUNEL assay was performed using the Apoptag Plus Peroxidase *In Situ* Apoptotic Detection Kit (Millipore) according to the manufacturer's instructions. Images were taken using a Leica DM 2000 LED microscope equipped with a Leica DFC450 C camera. All images were processed using ImageJ.

Animal studies

Six- to 10-week-old athymic nu/nu nude mice (Charles River Laboratories) were injected into the left flank with 2 million U937 cells. Once tumors reached a measurable size, mice were injected intraperitoneally daily with control (PBS with 5% DMSO), A769662 (Chemietek) at 30 mg/kg, As_2O_3 (pharmaceutical grade TRISENOX, Teva Pharmaceutical Industries Ltd) at 5 mg/kg, or the combination of A769662 with As_2O_3. We measured tumor length and width every 2 days and calculated volume with the formula $(D \times d^2)/2$, where D is the longest diameter and d is the shorter diameter Survival was measured as time to euthanasia. The criterion used for euthanasia was weight loss greater than 20%, tumor size exceeding 1.5 cm^3, or bleeding/eruption at the tumor site. All animal studies were approved by the Northwestern University Institutional Animal Care and Use Committee.

Statistical analysis

All statistical analyses were performed using Prism Graphpad 6.0.

Results

AMPK activity is inhibited by arsenic trioxide

It has been previously shown that the mTOR pathway is activated in response to treatment of AML cells with As_2O_3 and plays a negative regulatory role in the generation of antileukemic effects (34). As AMPK is a negative regulator of mTOR, we sought to determine whether the engagement of the mTOR pathway by As_2O_3 could be mechanistically regulated by inhibition of AMPK activation, leading to activation of mTOR. Treatment of AML cells with As_2O_3 inhibited phosphorylation of the AMPKα subunit at Thr172, which is required for activation of the kinase (Fig. 1A). At the same time, phosphorylation at the inhibitory site Ser 485/491 (40) increased (Fig. 1A). Consistent with this, the phosphorylation of the AMPK substrate ACC decreased with time, when cells were treated with As_2O_3, reflecting a decrease in AMPK kinase activity (Fig. 1B).

In subsequent studies, we determined the mechanisms by which As_2O_3 blocks AMPK activity. It is well established that LKB1 is one of the main kinases responsible for activating AMPK (26). We hypothesized that this is possibly a direct effect of arsenic on AMPK, as the phosphorylation/activation of the upstream kinase LKB1 did not decrease before or at the time of suppression of AMPK activation, as reflected by the phosphorylation of LKB1 at site Thr189 (Fig. 1C). As AMPK phosphorylation/activation was inhibited in cells, we next examined whether arsenic can inhibit

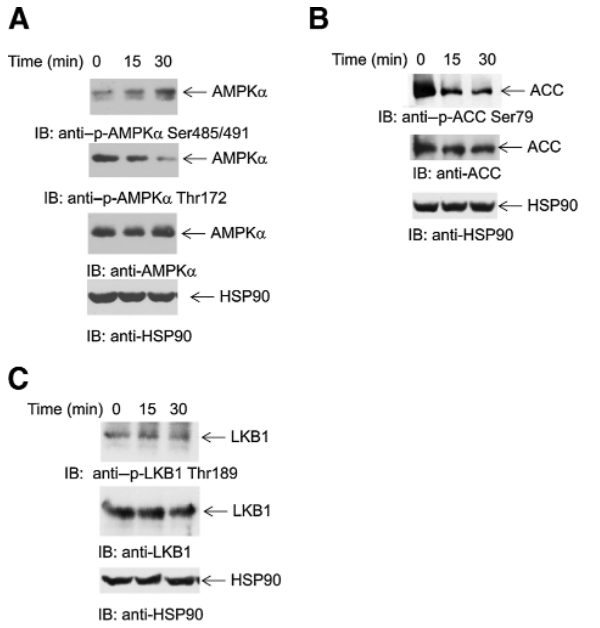

Figure 1.
Effects of As_2O_3 on AMPK phosphorylation in AML cells. U937 cells were treated with As_2O_3 (2 μmol/L) for the indicated times. Equal amounts of total cell lysates were subjected to SDS-PAGE followed by transfer to polyvinylidene difluoride membranes. Immunoblotting with the indicated antibodies against AMPKα (A), ACC (B), and LKB1 (C) and anti-HSP90 are shown. The immunoblots with antibodies against the phosphorylated forms of the proteins or against the total proteins were from lysates from the same experiments analyzed in parallel by SDS-PAGE.

AMPK kinase activity directly in an *in vitro* kinase assay (Fig. 2A). We pretreated active AMPK kinase with As_2O_3, the AMPK inhibitor compound C (41) or As-Biotin, before performing a kinase assay. Both As_2O_3 and As-Biotin significantly inhibited AMPK kinase activity *in vitro* (Fig. 2A), suggesting inhibitory effects via direct binding of arsenic to AMPK.

Arsenic binds directly to AMPK

To assess whether there is direct binding of arsenic to AMPK, we used an arsenic compound that is tagged with a biotin label, allowing its pulldown with streptavidin–agarose beads. AMPK recombinant protein was able to bind to the As-Biotin *in vitro* (Fig. 2B). In addition, we were able to show direct binding of AMPKα to As-Biotin in U937 cells, suggesting that arsenic modulates AMPK activity by direct binding (Fig. 2B). We then took advantage of the streptavidin pulldown to determine by mass spectroscopy where in the AMPKα sequence arsenic may bind. We chose to focus on the alpha subunit of AMPK because previously published data showed that two cysteines at residues 299 and 304 were important for activation of AMPK by oxidation (35). We treated AMPKα subunit alone or the AMPKα1/β1/γ1 holoenzyme with the As-Biotin compound and determined by mass spectroscopy that the biotin moiety was detected bound to cysteine 299 in AMPKα in both recombinant protein sources (Fig. 2C). It should be noted that this does not rule out the possibility that arsenic may be able to bind to other residues as they may have a lower binding affinity that cannot be detected by mass spectroscopy. To confirm these findings using a different approach, we overexpressed in HEK293 cells AMPKα wild-type (WT) or a mutant AMPKα in which both cysteines 299 and 304 were mutated to alanines. We were able to show that the mutant AMPKα does not bind as well to As-Biotin as the WT protein (Fig. 2D). Notably, binding was not completely abrogated by the mutation of cysteines 299 and 304, suggesting the existence of additional binding sites that might not have been detectable by mass spectroscopy.

Modulation of AMPK activity is important for the cytotoxic effects of As_2O_3

To examine the functional relevance of AMPK as a regulator of arsenic-dependent mTOR activation, we used embryonic fibroblasts from knockout mice for the AMPKα 1 and 2 isoforms (ref. 36; Supplementary Fig. S1A). In the absence of AMPK, treatment of the cells with As_2O_3 failed to induce activation/phosphorylation of the mTORC1 substrate S6K at Thr389 (Fig. 3A). However, the downstream effector of S6K, S6 ribosomal protein (rpS6) was still phosphorylated at Ser235/236 (Fig. 3B), suggesting the engagement of an alternative pathway that compensates for rpS6 phosphorylation. It has been previously shown that As_2O_3 activates the kinase RSK1 (ref. 18; Fig. 3B) and as RSK1 can phosphorylate rpS6 at this residue (42), we examined the possibility that RSK1 engagement is a mechanism for circumventing the loss of activation of mTOR signaling in the absence of AMPK. As expected, loss of AMPK did not eliminate the ability of As_2O_3 to activate mTORC2, as AKT phosphorylation at Ser473 was still detectable in AMPKα knockout cells (Supplementary Fig. S1B). Notably, the loss of AMPK led to reduced sensitivity to As_2O_3 as measured by a WST-1 viability assay (Fig. 3C and D). The IC_{50} for AMPK wild-type cells was 1.8 μmol/L versus 3.3 μmol/L for the AMPK knockout cells (Fig. 3C and D). We also calculated CI values to determine whether there were synergistic cytotoxic effects in combinations of As_2O_3 with either the catalytic mTOR inhibitor PP242 or the RSK inhibitor BI-D1870 (39). Cotreatment with PP242 only slightly enhanced As_2O_3-induced cytotoxicity in AMPKα knockout cells (CI value 0.99, consistent with additive effects; Fig. 3C). On the other hand, there was synergism between As_2O_3 and PP242 in AMPK wild-type cells (CI value 0.42; Fig. 3C). The presence of additive effects, but not synergy in the knockout cells is probably due to the fact that As_2O_3 is still able to activate mTORC2 activity that is not affected by the knockdown of AMPK. However, the opposite was seen when the RSK inhibitor BI-D1870 was used as the CI value for the wild-type cells is 1.00 indicating additive effects and the CI value for the knockout cells are 0.84 indicating synergistic effects (Fig. 3D).

We next sought to determine the effects of AMPK knockdown on the induction of the antileukemic properties of arsenic, as assessed by its ability to suppress the growth of primitive AML leukemic precursors (CFU-L). Knockdown of AMPKα1 resulted in a statistically significant antagonism of the antileukemic effects of arsenic on both U937- and Kasumi-1– derived leukemic progenitors, indicating that AMPK is required for generation of the suppressive effects of arsenic on leukemic precursors (Fig. 4A and B). Importantly, when the effects of siRNA-mediated knockdown of AMPKα1 in the generation of the effects of As_2O_3 on primary primitive leukemic precursors from patients with AML was examined, we found that the antileukemic effects of As_2O_3 were also reversed by targeting AMPKα1 (Fig. 4C), establishing a key role for AMPK modulation in the induction of As_2O_3-generated antileukemic effects.

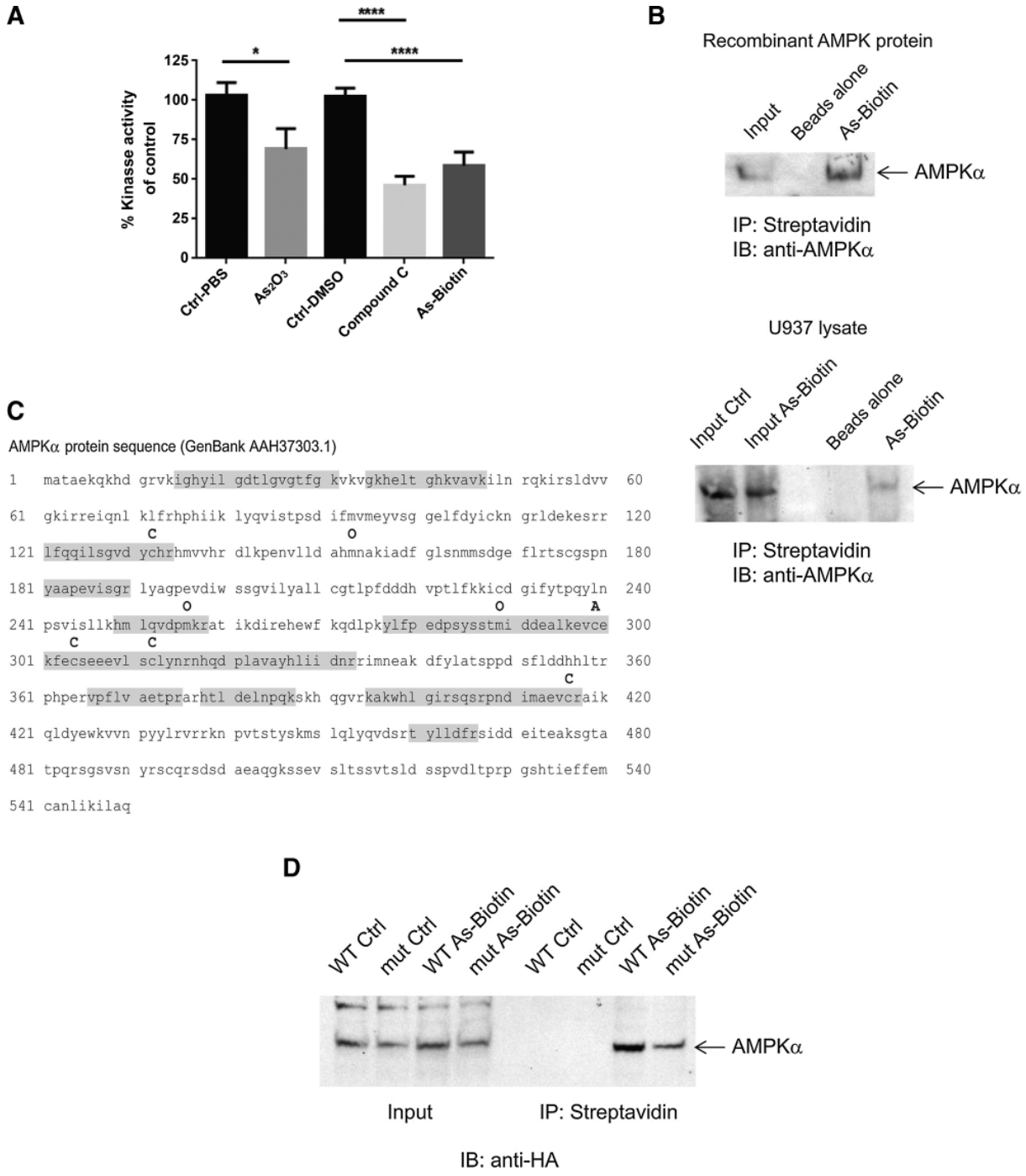

Figure 2.
Arsenic binds directly to AMPK and inhibits its kinase activity. A, an AMPK kinase assay was performed with AMPKα1/β1/γ1 recombinant protein using an ADP-Glo kinase assay. Drugs were used at a final concentration of 3 μmol/L. *, $P < 0.05$; ****, $P < 0.0001$ using an unpaired t test. B, recombinant AMPK protein was treated for 30 minutes at 30°C with As-Biotin (20 μmol/L) to assess in vitro binding of arsenic to AMPK. For in-cell binding experiments, U937 cells were treated with As-Biotin (20 μmol/L) for 2 hours and subsequently lysed. As-Biotin complexes were incubated with streptavidin beads overnight and then washed and eluted from the beads with 2× Laemelli sample buffer. Samples were then subjected to SDS-PAGE, followed by immunoblotting for AMPKα. C, mass spectroscopy was performed on recombinant AMPK protein and As-Biotin complexes. Shown is the AMPKα protein sequence annotated with the modifications found. C, cysteine unmodified; O, oxidation; and A, cysteine with As-Biotin. Highlighted in gray is the peptide coverage. D, HA-tagged AMPKα WT and AMPKα C299, 304A mutant proteins were overexpressed in HEK293 cells. Cells were treated with 20 μmol/L As-Biotin for 2 hours and subsequently lysed. Arsenic–protein complexes were isolated by incubation with streptavidin beads overnight and then washed and eluted from the beads with 2× Laemelli sample buffer. Samples were then subjected to SDS-PAGE, followed by Western blotting for HA tag.

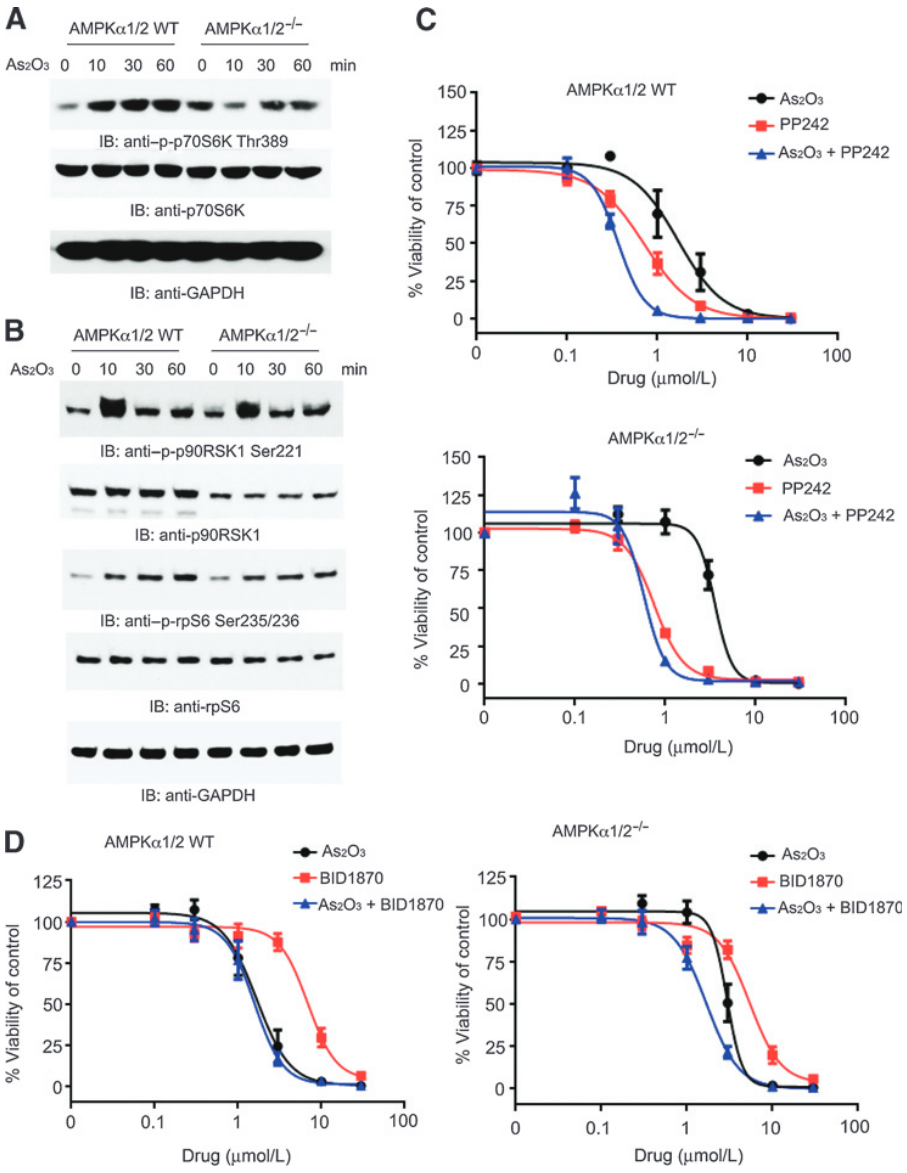

Figure 3.
Loss of AMPK affects arsenic-dependent signals and induction of cytotoxicity. A, AMPK 1/2 WT and knockout MEFs were serum starved overnight and then treated with As_2O_3 (5 μmol/L) for the indicated times. Total cell lysates were then resolved by SDS-PAGE and immunoblotted with the indicated antibodies. The immunoblots with antibodies against the phosphorylated forms of the proteins or against the total proteins were from lysates from the same experiments analyzed in parallel by SDS-PAGE. B, AMPK 1/2 WT and knockout MEFs were serum starved overnight and then treated with As_2O_3 (5 μmol/L) for the indicated times. Total cell lysates were then resolved by SDS-PAGE and immunoblotted with the indicated antibodies. The immunoblots with antibodies against the phosphorylated forms of the proteins or against the total proteins were from lysates from the same experiments analyzed in parallel by SDS-PAGE. The blots shown are the same lysates shown in A but were run in a different gel. C, AMPKα 1/2 WT and knockout MEFs were plated in 96-well plates and treated with varying concentrations of As_2O_3, the mTOR inhibitor PP242 and As_2O_3 + PP242 for 4 days. Viability was assessed using a WST-1 assay. Data are expressed as a percentage of vehicle control–treated cells. Shown are means and SEs of three independent experiments. D, AMPKα 1/2 WT and knockout MEFs were treated with varying concentrations of As_2O_3, or the RSK inhibitor BI-D1870 or the combination of As_2O_3 + BI-D1870 for 4 days and viability was measured by a WST-1 assay. Data are expressed as a percentage of vehicle control–treated cells. Shown are the means and SEs of three independent experiments.

The AMPK activator A769662 antagonizes the effects of ATO in vitro and in vivo

As we present data that arsenic can inhibit AMPK and that this is required in part for its antileukemic effects, we pursued further studies aimed to examine the effects of combining an AMPK activator with arsenic. We used the direct AMPK activator A769662 (43) as other activators such as metformin may have effects in cells independent of AMPK (44–46). In a cell viability assay, A769662 antagonized the effects of As_2O_3 (Fig. 5A). The IC_{50} for As_2O_3 alone was 1.64 μmol/L versus 2.33 μmol/L for the

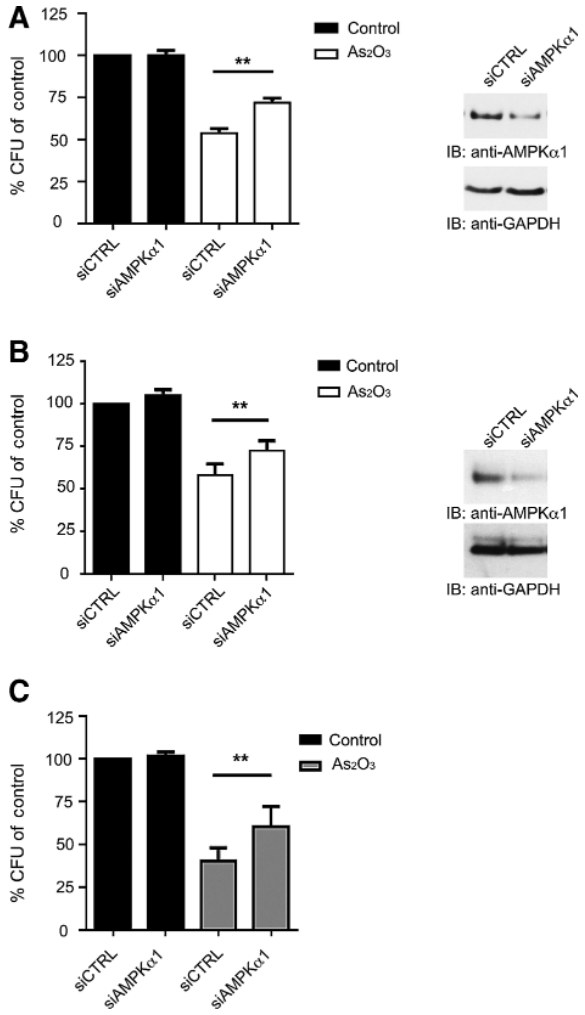

Figure 4.
Knockdown of AMPKα1 antagonizes the antileukemic effects of arsenic. A, U937 cells were transfected with AMPKα1 siRNA and then plated in methylcellulose in the presence or absence of As_2O_3 (1 μmol/L) and leukemic progenitor colony formation (CFU-L) was assessed in clonogenic assays in methylcellulose (left). Data are expressed as a percentage of the untreated control siRNA–transfected cells. Shown are the means +SE of six independent experiments. **, P < 0.01, using a paired t test. Right, immunblotting for AMPKα1 expression in total cell lysates from U937 cells transfected with control siRNA or AMPKα1 siRNA is shown. B, Kasumi-1 cells were transfected with AMPKα1 siRNA and then plated in methylcellulose in the presence or absence of As_2O_3 (1 μmol/L) and leukemic progenitor colony formation (CFU-L) was assessed in clonogenic assays in methylcellulose (left). Data are expressed as a percentage of the untreated control siRNA–transfected cells. Shown are the means +SE of six independent experiments. **, P < 0.01, using a paired t test. Right, immunblotting for AMPKα1 expression in total cell lysates from Kasumi-1 cells transfected with control siRNA or AMPKα1 siRNA is shown. C, mononuclear cells isolated from patients with AML were plated in clonogenic assays in methylcellulose to assess the effects of siRNA-mediated AMPKα1 knockdown in the generation of the suppressive effects of As_2O_3 (0.5 μmol/L) on primary leukemic progenitor colony formation (CFU-L). Data are expressed as a percentage of the untreated control siRNA–transfected cells. Shown are the means +SE of nine experiments performed with samples from different patients with AML.
**, P < 0.01 using a paired t test.

As_2O_3 + A769662 combination. The CI value was 1.66 indicating antagonism. In methylcellulose colony-forming assays, A769662 also antagonized the antileukemic effects of As_2O_3 on U937-derived leukemic progenitors (CFU-L; Fig. 5B) and on primary leukemic progenitors from patients with AML (Fig. 5C). We also examined whether A769662 was able to antagonize the effects of As_2O_3 on AMPK inhibition (Fig. 5D and E). The As_2O_3-dependent suppression of AMPKα phosphorylation at Thr172 (Fig. 5D) as well as the phosphorylation of the AMPK substrate ULK at Ser555 in U937 cells (Fig. 5E) were partially reversed by cotreatment with A769662, suggesting a mechanism for the reversal of the antileukemic effects of As_2O_3 by A769662.

In subsequent studies, we utilized a xenograft AML model to examine the effects of the combination of the AMPK activator with As_2O_3 *in vivo* (Fig. 6). A769662 alone did not significantly increase survival more than the control group. As expected, As_2O_3 was able to significantly increase survival with a *P* value of 0.0026 (Fig. 6A). However, such an As_2O_3 effect on survival was reversible by the combination of As_2O_3 with A769662, indicating that AMPK activation antagonizes the antineoplastic properties of As_2O_3 *in vivo*. Xenograft tumors from mice treated with control, A769662, As_2O_3, and A769662 + As_2O_3 were compared by histology and immunohistochemistry(IHC) for TUNEL staining as a measure of apoptosis (Fig. 6B). We compared the amount of necrosis between the tumors as As_2O_3 has been previously shown to induce marked necrosis in other xenograft models (22). The tumors of mice treated with As_2O_3 showed a statistically significant increase in necrosis compared with control mice, whereas none of the other treatment groups were statistically different than the control group (Fig. 6B and C). There was no significant difference in the morphology of the tumors in viable tumor areas, and the As_2O_3-treated tumors showed a trend toward increased apoptosis by TUNEL staining compared with the control tumors; however, this was not statistically significant (Fig. 6B).

Discussion

There has been extensive evidence documenting the potent antineoplastic properties of arsenic trioxide and other arsenicals *in vitro* and *in vivo* (3), but the mechanisms accounting for these antineoplastic activities remain to be precisely established. In the current study, we provide evidence for a unique mechanism by which As_2O_3 modulates activation of mTOR, involving inhibition of AMPK kinase activity via direct binding to cysteine 299 in the kinase. Cysteine 299 was one of the residues shown to be important for activation of AMPK activation by oxidation (35). Therefore, we propose that arsenic inhibits activation of AMPK by preventing oxidation of this cysteine residue.

It has been previously proposed that AMPK activation by oxidation is secondary to phosphorylation at Thr172, based on findings demonstrating no effects on AMPK phosphorylation at the T-loop in response to hydrogen peroxide, by mutation of cysteines 299 and 304 (35). However, in our study which involved assessment of responses after As_2O_3 treatment, we found that there is clearly an As_2O_3-dependent decrease in phosphorylation at Thr172 and this was accompanied by an increase in phosphorylation at the inhibitory site Ser485/489. This site has been proposed to be both an autophosphorylation site as well as directly targeted by AKT and PKA and leads to inhibition of AMPK activity by preventing phosphorylation of Thr172 (40, 47, 48). Binding of arsenic to cysteines in proteins was previously shown

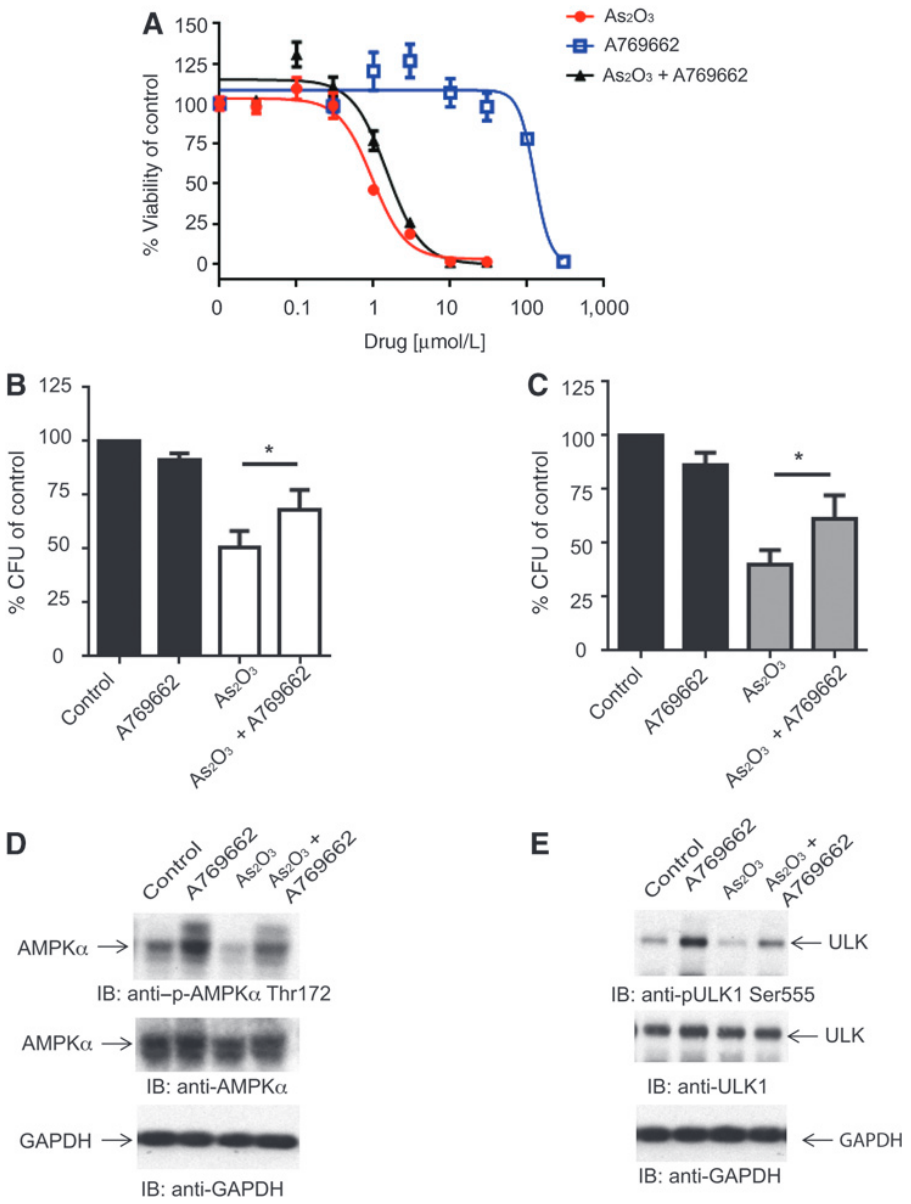

Figure 5.
Cotreatment with the direct AMPK activator A769662 antagonizes the cytotoxic effects of As_2O_3 in vitro. A, U937 cells were treated with varying concentrations of As_2O_3, A769662 or As_2O_3 + A769662 for 4 days and viability was assessed by a WST-1 assay. Data are expressed as a percentage of vehicle control–treated cells. Shown are means +SE of three independent experiments. B, U937 cells were plated in clonogenic assays in methylcellulose in the presence of As_2O_3 (1 μmol/L), A769662 (200 μmol/L), or As_2O_3 +A769662, as indicated and CFU-L leukemic colony formation was assessed. Shown are means +SE of six independent experiments. *, $P < 0.05$ using a paired t test. C, mononuclear cells isolated from patients with AML were plated in clonogenic assays in methylcellulose in the presence of As_2O_3 (1 μmol/L), A769662 (200 μmol/L), or As_2O_3 +A769662, as indicated and primary leukemic progenitor colony formation (CFU-L) was assessed. Shown are the means +SE of eight experiments performed with samples from different AML patients. *, $P < 0.05$ using a paired t test. D, U937 cells were treated with As_2O_3 (2 μmol/L), A769662 (300 μmol/L), or As_2O_3 + A769662 for 2 hours. Total cell lysates were resolved by SDS-PAGE and immunoblotted with the indicated antibodies. The immunoblots with antibodies against the phosphorylated forms of the proteins or against the total proteins were from lysates from the same experiments analyzed in parallel by SDS-PAGE. E, U937 cells were treated with As_2O_3 (2 μmol/L), A769662 (300 μmol/L), or As_2O_3 +A769662 for 2 hours. Total cell lysates were resolved by SDS-PAGE and immunoblotted with the indicated antibodies. The immunoblots with antibodies against the phosphorylated forms of the proteins or against the total proteins were from lysates from the same experiments analyzed in parallel by SDS-PAGE.

to alter protein confirmation and secondary structure (8, 49). Thus, it is possible that in addition to preventing oxidation, binding of arsenic to AMPK causes a structural conformation change that promotes binding of PKA or AKT, allowing phosphorylation of Ser495/489 and inhibition of Thr172 phosphorylation. Another report has shown that arsenic can inhibit the

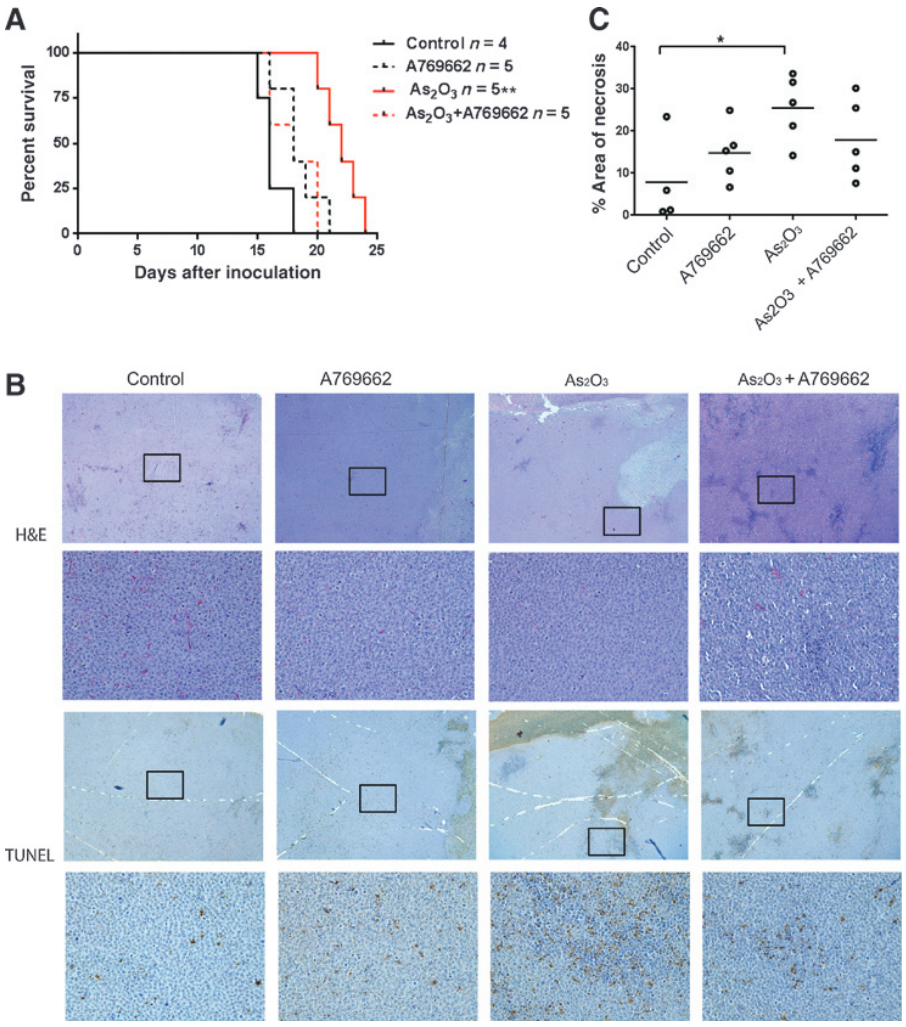

Figure 6.
A769662 antagonizes the effects of As_2O_3 in vivo. A, U937 cells were injected into the left flank of athymic nude mice. The indicated numbers of animals were treated with control, A769662, As_2O_3, and the combination of As_2O_3 + A769662. Survival was determined as the time to euthanasia. **, $P < 0.01$, using a log-rank (Mantel–Cox) test. B, tumors from the mice in A were analyzed by hematoxylin and eosin (H&E) and IHC for TUNEL as a marker of apoptosis. Boxed regions show viable cells presented at higher magnification in the images below. Magnification: top, ×25; bottom, ×200. C, the percentage area of necrosis was measured from 5 different fields covering a majority of the tumor sample at ×25 magnification. Area was measured using ImageJ. *, $P < 0.05$, using a one-way ANOVA analysis with a Bonferroni correction.

LKB1–AMPK pathway, leading to a reduction in neurite outgrowth (50). The authors attributed that to an effect of arsenic on LKB1 activation as they saw simultaneous inhibition of LKB1 and AMPK. We, however, did not see simultaneous effects and instead found inhibition of AMPK before effects on LKB1 phosphorylation, indicating that the effects of arsenic reflect direct binding to AMPK. The difference between the previous study and ours may be due to differences in cell types studied, but likely reflect the delayed assessment of effects in that study, done after 24 or 48 hours after treatment.

AMPK is historically thought of as a tumor suppressor, but recent evidence has suggested that, depending on context, it may function as an oncogene (51). Specifically, AMPK was recently shown to regulate NADPH and ROS levels in tumor cells to promote survival during energy stress (52). Our findings that AMPK inhibition by arsenic is required in part for its cytotoxic effects on both AML lines and primary leukemic progenitors from AML patients are consistent with a potential oncogenic role for AMPK. The production of ROS by arsenic is very important for its cytotoxic effects (3) and it is possible that part of its ability to increase ROS in the cell may be through inhibition of AMPK, leading to suppression of proliferation and inhibitory effects on leukemic progenitor colony formation. Activation of AMPK by A769662 may antagonize the production of ROS by arsenic and lead to decreased cytotoxic effects when the two agents are combined.

Recent data have suggested that activation of AMPK by metformin is a potential therapeutic target in AML (53). Interestingly, the direct AMPK activator A769662 alone had no effect alone in the xenograft model of AML and did not inhibit proliferation

in vitro until high doses (Figs. 5 and 6). Others have shown that direct AMPK activation by A769662 did not inhibit proliferation of glioma cells, whereas AICAR and metformin were able to do so, and attributed this to the AMPK-independent effects of both drugs (46). In addition, a recent study showed that phenformin (a metformin analog) was most effective in LKB1-inactivated lung tumors (54). In this setting, the drug failed to activate AMPK as the cells lacked the upstream kinase LKB1 but was more effective in its cytotoxic effects through AMPK-independent pathways such as eIF2α, CHOP, and mitochondrial membrane potential (54). Therefore, it is possible that the antitumorigenic effects of metformin occur to a large extent via AMPK-independent mechanisms. Future clinical–translational efforts should also take into consideration the fact that direct activation of AMPK may not have significant effects therapeutically in AML, and, in fact, AMPK activation may be oncogenic and/or antagonize the antileukemic effects of other agents such as arsenic trioxide.

Disclosure of Potential Conflicts of Interest

No potential conflicts of interest were disclosed..

Authors' Contributions

Conception and design: E. Beauchamp, E.P. Swindell, T.V. O'Halloran, L.C. Platanias

Development of methodology: E. Beauchamp, E.P. Swindell

Acquisition of data (provided animals, acquired and managed patients, provided facilities, etc.): E. Beauchamp, E.M. Kosciuczuk, D. Nanavati, B. Viollet, J.K. Altman

Analysis and interpretation of data (e.g., statistical analysis, biostatistics, computational analysis): E. Beauchamp, E.M. Kosciuczuk, R. Serrano, D. Nanavati, L.C. Platanias

Writing, review, and/or revision of the manuscript: E. Beauchamp, E.P. Swindell, B. Viollet, T.V. O'Halloran, L.C. Platanias

Acknowledgments

The authors thank Anne Brunet and Bethany E. Schaffer (Stanford University, Stanford, CA) for providing the pECE-AMPKα1 WT construct.

Grant Support

The work was supported in part by NIH grants CA121192, CA77816, and CA155566 (to L.C. Platanias) and grant I01CX000916 from the Department of Veterans Affairs (to L.C. Platanias). E.M. Beauchamp was supported in part by NIH training grants T32CA070085 and F32CA183536.

The costs of publication of this article were defrayed in part by the payment of page charges. This article must therefore be hereby marked *advertisement* in accordance with 18 U.S.C. Section 1734 solely to indicate this fact.

Received August 8, 2014; revised September 24, 2014; accepted October 12, 2014; published OnlineFirst October 24, 2014.

References

1. Waxman S, Anderson KC. History of the development of arsenic derivatives in cancer therapy. Oncologist 2001;6 Suppl 2:3–10.
2. Cohen MH, Hirschfeld S, Flamm Honig S, Ibrahim A, Johnson JR, O'Leary JJ, et al. Drug approval summaries: arsenic trioxide, tamoxifen citrate, anastrazole, paclitaxel, bexarotene. Oncologist 2001;6:4–11.
3. Platanias LC. Biological responses to arsenic compounds. J Biol Chem 2009;284:18583–7
4. Dilda PJ, Hogg PJ. Arsenical-based cancer drugs. Cancer Treat Rev 2007;33:542–64.
5. Ramadan D, Rancy PC, Nagarkar RP, Schneider JP, Thorpe C. Arsenic(III) species inhibit oxidative protein folding in vitro. Biochemistry 2009;48: 424–32.
6. Swindell EP, Hankins PL, Chen H, Miodragovic DU, O'Halloran TV. Anticancer activity of small-molecule and nanoparticulate arsenic(III) complexes. Inorg Chem 2013;52:12292–304.
7. Nasr R, Guillemin MC, Ferhi O, Soilihi H, Peres L, Berthier C, et al. Eradication of acute promyelocytic leukemia-initiating cells through PML-RARA degradation. Nat Med 2008;14:1333–42.
8. Zhang XW, Yan XJ, Zhou ZR, Yang FF, Wu ZY, Sun HB, et al. Arsenic trioxide controls the fate of the PML-RARalpha oncoprotein by directly binding PML. Science 2010;328:240–3.
9. Goussetis DJ, Gounaris E, Wu EJ, Vakana E, Sharma B, Bogyo M, et al. Autophagic degradation of the BCR-ABL oncoprotein and generation of antileukemic responses by arsenic trioxide. Blood 2012;120: 3555–62.
10. Shackelford D, Kenific C, Blusztajn A, Waxman S, Ren R. Targeted degradation of the AML1/MDS1/EVI1 oncoprotein by arsenic trioxide. Cancer Res 2006;66:11360–9.
11. Kapahi P, Takahashi T, Natoli G, Adams SR, Chen Y, Tsien RY, et al. Inhibition of NF-kappa B activation by arsenite through reaction with a critical cysteine in the activation loop of Ikappa B kinase. J Biol Chem 2000;275:36062–6.
12. Giafis N, Katsoulidis E, Sassano A, Tallman MS, Higgins LS, Nebreda AR, et al. Role of the p38 mitogen-activated protein kinase pathway in the generation of arsenic trioxide-dependent cellular responses. Cancer Res 2006;66:6763–71.
13. Dolniak B, Katsoulidis E, Carayol N, Altman JK, Redig AJ, Tallman MS, et al. Regulation of arsenic trioxide-induced cellular responses by Mnk1 and Mnk2. J Biol Chem 2008;283:12034–42.
14. Kannan-Thulasiraman P, Katsoulidis E, Tallman MS, Arthur JS, Platanias LC. Activation of the mitogen- and stress-activated kinase 1 by arsenic trioxide. J Biol Chem 2006;281:22446–52.
15. Verma A, Mohindru M, Deb DK, Sassano A, Kambhampati S, Ravandi F, et al. Activation of Rac1 and the p38 mitogen-activated protein kinase pathway in response to arsenic trioxide. J Biol Chem 2002;277:44988–95.
16. Goussetis DJ, Altman JK, Glaser H, McNeer JL, Tallman MS, Platanias LC. Autophagy is a critical mechanism for the induction of the antileukemic effects of arsenic trioxide. J Biol Chem 2010;285:29989–97.
17. Hayakawa F, Privalsky ML. Phosphorylation of PML by mitogen-activated protein kinases plays a key role in arsenic trioxide-mediated apoptosis. Cancer Cell 2004;5:389–401.
18. Galvin JP, Altman JK, Szilard A, Goussetis DJ, Vakana E, Sassano A, et al. Regulation of the kinase RSK1 by arsenic trioxide and generation of antileukemic responses. Cancer Biol Ther 2013;14:411–6.
19. Davison K, Mann KK, Waxman S, Miller WH Jr. JNK activation is a mediator of arsenic trioxide-induced apoptosis in acute promyelocytic leukemia cells. Blood 2004;103:3496–502.
20. Mann KK, Davison K, Colombo M, Colosimo AL, Diaz Z, Padovani AM, et al. Antimony trioxide-induced apoptosis is dependent on SEK1/JNK signaling. Toxicol Lett 2006;160:158–70.
21. Redondo-Munoz J, Escobar-Diaz E, Hernandez Del Cerro M, Pandiella A, Terol MJ, Garcia-Marco JA, et al. Induction of B-chronic lymphocytic leukemia cell apoptosis by arsenic trioxide involves suppression of the phosphoinositide 3-kinase/Akt survival pathway via c-jun-NH2 terminal kinase activation and PTEN upregulation. Clin Cancer Res 2010;16: 4382–91.
22. Beauchamp EM, Ringer L, Bulut G, Sajwan KP, Hall MD, Lee YC, et al. Arsenic trioxide inhibits human cancer cell growth and tumor development in mice by blocking Hedgehog/GLI pathway. J Clin Invest 2011;121:148–60.
23. Fei DL, Li H, Kozul CD, Black KE, Singh S, Gosse JA, et al. Activation of Hedgehog signaling by the environmental toxicant arsenic may contribute to the etiology of arsenic-induced tumors. Cancer Res 2010;70:1981–8.
24. Kim J, Lee JJ, Gardner D, Beachy PA. Arsenic antagonizes the Hedgehog pathway by preventing ciliary accumulation and reducing stability of the Gli2 transcriptional effector. Proc Natl Acad Sci U S A 2010;107:13432–7.
25. Carling D, Mayer FV, Sanders MJ, Gamblin SJ. AMP-activated protein kinase: nature's energy sensor. Nat Chem Biol 2011;7:512–8.

26. Woods A, Vertommen D, Neumann D, Turk R, Bayliss J, Schlattner U, et al. Identification of phosphorylation sites in AMP-activated protein kinase (AMPK) for upstream AMPK kinases and study of their roles by site-directed mutagenesis. J Biol Chem 2003;278:28434–42.
27. Hawley SA, Davison M, Woods A, Davies SP, Beri RK, Carling D, et al. Characterization of the AMP-activated protein kinase kinase from rat liver and identification of threonine 172 as the major site at which it phosphorylates AMP-activated protein kinase. J Biol Chem 1996;271: 27879–87.
28. Hurley RL, Anderson KA, Franzone JM, Kemp BE, Means AR, Witters LA. The Ca2+/Calmodulin-dependent protein kinase kinases are AMP-activated protein kinase kinases. J Biol Chem 2005;280:29060–6.
29. Shaw RJ, Kosmatka M, Bardeesy N, Hurley RL, Witters LA, DePinho RA, et al. The tumor suppressor LKB1 kinase directly activates AMP-activated kinase and regulates apoptosis in response to energy stress. Proc Natl Acad Sci U S A 2004;101:3329–35.
30. Davies SP, Carling D, Munday MR, Hardie DG. Diurnal rhythm of phosphorylation of rat liver acetyl-CoA carboxylase by the AMP-activated protein kinase, demonstrated using freeze-clamping. Effects of high fat diets. Eur J Biochem 1992;203:615–23.
31. Inoki K, Kim J, Guan KL. AMPK and mTOR in cellular energy homeostasis and drug targets. Annu Rev Pharmacol Toxicol 2012;52:381–400.
32. Egan D, Kim J, Shaw RJ, Guan KL. The autophagy initiating kinase ULK1 is regulated via opposing phosphorylation by AMPK and mTOR. Autophagy 2011;7:643–4.
33. Beauchamp EM, Platanias LC. The evolution of the TOR pathway and its role in cancer. Oncogene 2013;32:3923–32.
34. Altman JK, Yoon P, Katsoulidis E, Kroczynska B, Sassano A, Redig AJ, et al. Regulatory effects of mammalian target of rapamycin-mediated signals in the generation of arsenic trioxide responses. J Biol Chem 2008;283: 1992–2001.
35. Zmijewski JW, Banerjee S, Bae H, Friggeri A, Lazarowski ER, Abraham E. Exposure to hydrogen peroxide induces oxidation and activation of AMP-activated protein kinase. J Biol Chem 2010;285:33154–64.
36. Laderoute KR, Amin K, Calaoagan JM, Knapp M, Le T, Orduna J, et al. 5′-AMP-activated protein kinase (AMPK) is induced by low-oxygen and glucose deprivation conditions found in solid-tumor microenvironments. Mol Cell Biol 2006;26:5336–47.
37. Moaddel R, Sharma A, Huseni T, Jones GS Jr, Hanson RN, Loring RH. Novel biotinylated phenylarsonous acids as bifunctional reagents for spatially close thiols: studies on reduced antibodies and the agonist binding site of reduced Torpedo nicotinic receptors. Bioconjug Chem 1999;10:629–37.
38. Zhang X, Yang F, Shim JY, Kirk KL, Anderson DE, Chen X. Identification of arsenic-binding proteins in human breast cancer cells. Cancer Lett 2007;255:95–106.
39. Chou TC. Theoretical basis, experimental design, and computerized simulation of synergism and antagonism in drug combination studies. Pharmacol Rev 2006;58:621–81.
40. Hurley RL, Barre LK, Wood SD, Anderson KA, Kemp BE, Means AR, et al. Regulation of AMP-activated protein kinase by multisite phosphorylation in response to agents that elevate cellular cAMP. J Biol Chem 2006;281: 36662–72.
41. Zhou G, Myers R, Li Y, Chen Y, Shen X, Fenyk-Melody J, et al. Role of AMP-activated protein kinase in mechanism of metformin action. J Clin Invest 2001;108:1167–74.
42. Roux PP, Shahbazian D, Vu H, Holz MK, Cohen MS, Taunton J, et al. RAS/ERK signaling promotes site-specific ribosomal protein S6 phosphorylation via RSK and stimulates cap-dependent translation. J Biol Chem 2007;282:14056–64.
43. Cool B, Zinker B, Chiou W, Kifle L, Cao N, Perham M, et al. Identification and characterization of a small molecule AMPK activator that treats key components of type 2 diabetes and the metabolic syndrome. Cell Metab 2006;3:403–16.
44. El-Mir MY, Nogueira V, Fontaine E, Averet N, Rigoulet M, Leverve X. Dimethylbiguanide inhibits cell respiration via an indirect effect targeted on the respiratory chain complex I. J Biol Chem 2000;275:223–8.
45. Kalender A, Selvaraj A, Kim SY, Gulati P, Brule S, Viollet B, et al. Metformin, independent of AMPK, inhibits mTORC1 in a rag GTPase-dependent manner. Cell Metab 2010;11:390–401.
46. Liu X, Chhipa RR, Pooya S, Wortman M, Yachyshin S, Chow LM, et al. Discrete mechanisms of mTOR and cell cycle regulation by AMPK agonists independent of AMPK. Proc Natl Acad Sci U S A 2014;111:E435–44.
47. Horman S, Vertommen D, Heath R, Neumann D, Mouton V, Woods A, et al. Insulin antagonizes ischemia-induced Thr172 phosphorylation of AMP-activated protein kinase alpha-subunits in heart via hierarchical phosphorylation of Ser485/491. J Biol Chem 2006;281:5335–40.
48. Soltys CL, Kovacic S, Dyck JR. Activation of cardiac AMP-activated protein kinase by LKB1 expression or chemical hypoxia is blunted by increased Akt activity. Am J Physiol Heart Circ Physiol 2006;290:H2472–9.
49. Cline DJ, Thorpe C, Schneider JP. Effects of As(III) binding on alpha-helical structure. J Am Chem Soc 2003;125:2923–9.
50. Wang X, Meng D, Chang Q, Pan J, Zhang Z, Chen G, et al. Arsenic inhibits neurite outgrowth by inhibiting the LKB1-AMPK signaling pathway. Environ Health Perspect 2010;118:627–34.
51. Liang J, Mills GB. AMPK: a contextual oncogene or tumor suppressor? Cancer Res 2013;73:2929–35.
52. Jeon SM, Chandel NS, Hay N. AMPK regulates NADPH homeostasis to promote tumour cell survival during energy stress. Nature 2012;485: 661–5.
53. Green AS, Chapuis N, Maciel TT, Willems L, Lambert M, Arnoult C, et al. The LKB1/AMPK signaling pathway has tumor suppressor activity in acute myeloid leukemia through the repression of mTOR-dependent oncogenic mRNA translation. Blood 2010;116:4262–73.
54. Shackelford DB, Abt E, Gerken L, Vasquez DS, Seki A, Leblanc M, et al. LKB1 inactivation dictates therapeutic response of non-small cell lung cancer to the metabolism drug phenformin. Cancer Cell 2013;23:143–58.